Accepted Manuscript

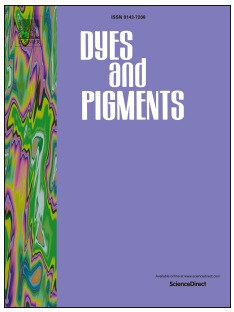

A neutral pH probe of rhodamine derivatives inspired by effect of hydrogen bond on pKa and its organelle-targetable fluorescent imaging

Haibo Yu, Guli Li, Bei Zhang, Xinfu Zhang, Yi Xiao, Jieqiong Wang, Youtao Song

PII: S0143-7208(16)30218-2

DOI: 10.1016/j.dyepig.2016.05.028

Reference: DYPI 5260

To appear in: *Dyes and Pigments*

Received Date: 22 April 2016

Revised Date: 13 May 2016

Accepted Date: 18 May 2016

Please cite this article as: Yu H, Li G, Zhang B, Zhang X, Xiao Y, Wang J, Song Y, A neutral pH probe of rhodamine derivatives inspired by effect of hydrogen bond on pKa and its organelle-targetable fluorescent imaging, *Dyes and Pigments* (2016), doi: 10.1016/j.dyepig.2016.05.028.

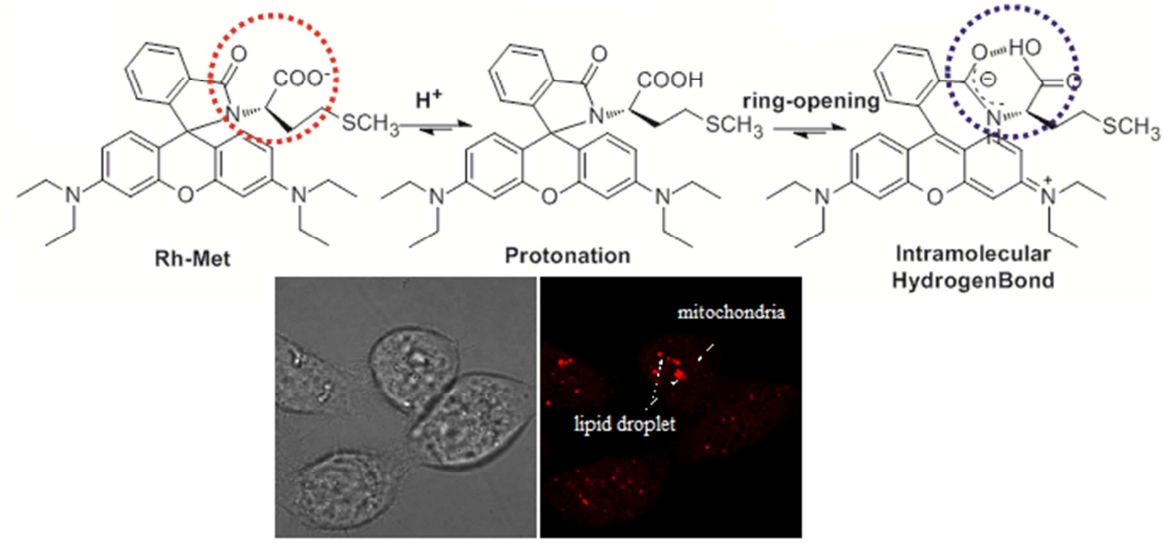

A neutral pH probe of rhodamine derivatives inspired by effect of hydrogen bond on pKa and its organelle-targetable fluorescent imaging

Haibo Yu,[a,b] Guli Li,[a] Bei Zhang,[c] Xinfu Zhang,[b] Yi Xiao,[b*] Jieqiong Wang,[a] Youtao Song[a**]

a.College of Environmental Sciences, Liaoning University, Shenyang 110036, P.R.China, email: yuhaibo@lnu.edu.cn

b.State Key Laboratory of Fine Chemicals, Dalian University of Technology, Dalian 116012,P .R. China.

c.Department of Chemistry, University of Kentucky, Lexington, Kentucky, 40506, USA

ARTICLEINFO

Article history:
xxxxxx

Keywords:
Fluorescent probe
Rhodamine spirolactam
Hydrogen bond
pH
Fluorescent imaging
Colorimetric

ABSTRACT

A neutral pH fluorescent probe (Rh-Met) based on rhodamine spirolactam is firstly developed according to the modulation strategy of hydrogen bonds on pKa values. The pKa value of Rh-Met was 6.81(±0.06) and higher than that of other rhodamine spirolactams known. Rh-Met showed a 240-fold enhancement of fluorescence intensity at 585 nm with attenuation of pH values from 9.7 to 3.5. In addition, Rh-Met displayed an excellent selectivity and reversible response to hydrogen ion. And it was successfully employed for imaging endocellular hydrogen ion in mitochondria and lipid droplets. These results suggested that Rh-Met could be a potential tool to assess pH fluctuation in mitochondria and lipid droplets, and would promote many new opportunities for studying the biological effect of pH in living cells.

1. Introduction

Hydrogen bonding force as an intermolecular interaction plays an important role in many chemical phenomena such as regulation of physicochemical properties (e.g. melting and boiling point, solubility, density, dielectricity, acid-base properties) [1], synthesis of polymer (nylon) and cellulose [2], infrared absorption spectrum [3], and determining structure of multimeric proteins and DNA [4]. In traditional textbooks, hydrogen bonding has been shown to affect the pKa value of many molecules such as phthalic acid, salicylic acid and maleic acid [1]. Compared with the pKa of fumaric acid (pKa1 3.02, pKa2 4.39), maleic acid has a much lower pKa1 of 2.0 and a higher pKa2 of 6.26, which indicates that the second acid dissociation at pH around 6.26 is more difficult, due to intramolecular hydrogen bonding formation [1], as shown in Scheme 1a. On the other hand, one of the carboxylate ions of maleate readily combines with hydrogen ion to form carboxylic acid at pH 6.26, and then the oxygen atoms with electronegative pairs in another carboxylate ion become quite prone to form

*Corresponding author. College of Environmental Sciences, Liaoning University, Shenyang 110036, P.R.China, Email: yuhaibo@lnu.edu.cn

intramolecular hydrogen bonding (Scheme1a). Recently, Steven R. Kass et al.[5] illustrated the effect of hydrogen bond on pKa value of acyclic aliphatic heptaol. The effect of hydrogen bond on pKa value has enormously captured our attentions.

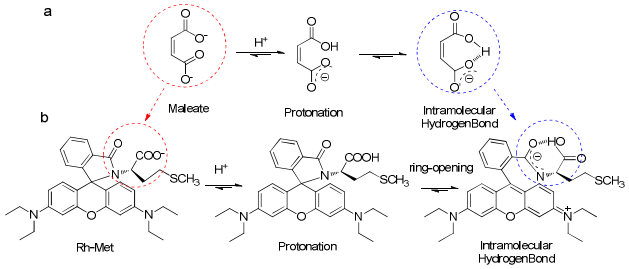

Scheme 1 Hydrogen bonding formation of Maleate (a) and Rh-Met (b) in the process of protonation

Owing to its excellent properties of ring switching and low background fluorescence, especially its pH insensitivity, rhodamine spirolactam has been widely utilized as a scaffold to design fluorescent probes for metal ions and reactive molecules in the past two decades [6-13].Precisely because of its acidic pKa value (4.0-6.0) and pH independence in the range from pH 6.0 to 10, rhodamine spirolactam has been a first-selection for designing fluorescent probe used in neutral aqueous solutions [14-25]. This advantage of rhodamine spirolactam limits, to some extent, its development of neutral pH fluorescent probes, though it is considered better as acid-sensitive fluorescent probes reported previously[26-31]. W. Lin et al. [32] have described a strategy to tune the pKa values of rhodamine derivatives based on rhodamine 6G by incorporating a steric group on the spirolactam moiety. However, that strategy seems to work very well for rhodamine 6G rather than for rhodamine B, due to higher sensitivity of rhodamine 6G derivatives. Although a number of lysosome-targetable fluorescent probes have been reported [33-36], the development of neutral pH fluorescent probe based on rhodamine B is still a great challenge.

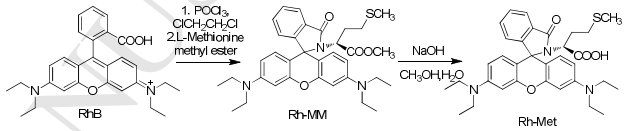

Scheme 2 Synthetic route of probe Rh-Met

In this paper a neutral pH fluorescent probe (Rh-Met) has been developed, in which L-methionine was tethered to rhodamine B through spirolactam. The synthetic route is shown in Scheme 2. As we know, the pKa of methionine is about 2.28, then the carboxylic acid will dissociate in neutral aqueous solutions. Similar to maleate, formylmethionate moiety of rhodamine spirolactam (Rh-Met) would show a homologous behaviour with decreasing pH values (Scheme 1b). It is possible that the regulative effect of hydrogen bond is also applicable to design neutral pKa fluorescent probes based on rhodamine B spirolactam.

2. Experimental

2.1 General methods and reagents

^{1}H-NMR and ^{13}C-NMR were measured on Varian MERCURY 300 spectrometer in $CDCl_3$ with TMS as internal reference. Mass spectra were measured on a HP 1100 LC-MSD, Gas chromatography/TOF Mass spectrometers and the UPLC/Q-TOF Mass spectrometers. Fluorescence spectra were measured on Spectrofluorophotometer (Cary Eclipse). Absorbance spectra were recorded on a UV-vis Spectrophotometer (TU-1901). An inverted confocal fluorescent microscopy (Olympus FV1000, IX81, Olympus, Japan) equipped with an objective lens (×100 oil, 1.4 Numerical Aperture (NA), Scan mode XY) was used in the imaging of living cells.

All reagents such as $ClCH_2CH_2Cl$, $POCl_3$, acetonitrile and triethylamine were purchased from commercial suppliers and used without further purification. Column chromatography was performed with silica gel (300-400 mesh). RPMI 1640 culture medium with L-glutamine, 4,4-Difluoro-1,3,5,7,8-Pentamethyl-4-Bora-3a,4a-Diaza-s-Indacene (BODIPY®493/503) and 3,6-diamino-9-[2-(methoxy-carbonyl)phenyl]-xanthylium chloride (rhodamine 123, Rh123) were purchased from GIBCO (Invitrogen, USA), FBS (fetal calf serum) was purchased from GIBCO (Invitrogen, USA).

2.2 Synthesis of Rh-MM

Rhodamine B acid chloride (RhB-Cl) was synthesized and obtained according to the procedure previously reported in literature.[14] A solution of Rhodamine B (RhB) (500 mg, 0.14 mmol) in dry 1,2-dichloroethane (50 mL) was stirred until the solid dissolved completely, and phosphorus oxychloride (0.28 mL) was added with vigorously stirring at room temperature for 5 min. Then the solution was refluxed for 5 h. The reaction mixture was cooled and used without further purification. A solution of methyl methionine (0.35 g, 0.16 mmol) and NEt_3 (2 mL) dissolved in CH_3CN (10 mL) was added dropwise to the solution above of crude acid chloride in 1,2-dichloroethane. After stirring over night, the crude product was purified through silica gel column chromatography with a mixture of dichloromethane and ethylene acetate (15:1, v/v) as eluent. Rh-MM was obtained as a colorless powder (52 mg, Yield 62.5%). ^{1}H NMR (300 MHz, $CDCl_3$) δ 7.91 (dd, 1H, J = 5.9, 2.9 Hz), 7.48 – 7.39 (m, 2H), 7.17–7.08 (m, 1H), 6.54 (d, 1H, J = 9.0 Hz), 6.43 (d, 1H, J = 9.0 Hz), 6.38 (t, 2H, J = 2.4 Hz), 6.27 (m, 2H), 3.83 (t, 1H, J = 6.0 Hz), 3.46 (s, 3H), 3.33 (q, 8H, J = 7.0 Hz), 2.34 – 2.18 (m, 2H), 2.13 – 2.01 (m, 2H), 1.77 (s, 3H), 1.21 – 1.10 (m, 12H).^{13}C NMR (75 MHz, $CDCl_3$) δ 170.8, 167.3, 153.7, 153.6, 152.8, 148.7, 132.5, 131.7, 130.7, 129.3, 128.1, 123.9, 122.8, 108.1, 107.4, 97.8, 77.4, 77.2, 76.9, 76.6, 65.8, 53.4, 51.8, 44.4, 31.2, 29.5, 14.7,

12.5. ESI-MS C34H41N3O4S Exact Mass: 587.2818, Found: 588.0307 ($[M+H]^+$).

2.3 Synthesis of Rh-Met

Rh-MM (100 mg, 0.17 mmol) and NaOH (70 mg, 1.75 mmol) was dissolved in methane-H_2O (5 mL / 5 mL) and refluxed for 7 h. After completion of the reaction (monitored via thin-layer chromatography), the methane was evaporated in vacuo. Rh-Met (80 mg, yield 82%) was obtained through silica gel column chromatography with a mixture of dichloromethane and methane (15:1, v/v) as eluent. ^{1}H NMR (300 MHz, $CDCl_3$) δ 7.91 (dd, 1H, *J* = 5.7, 2.8 Hz), 7.52 (dd, 2H, *J* = 6.2, 2.8 Hz), 7.13 (dd, 1H, *J* = 5.4, 2.5 Hz), 6.45 (d, 1H, *J* = 2.1 Hz), 6.42 (d, 1H, *J* = 2.1 Hz), 6.41 – 6.37 (m, 2H), 6.32 – 6.23 (m, 2H), 3.83 (dd, 1H, *J* = 9.2, 5.8 Hz), 3.33 (p, 8H, *J* = 6.9 Hz), 2.54 – 2.30 (m, 1H), 2.18 (t, 2H, *J* = 7.5 Hz), 1.91 – 1.73 (m, 4H), 1.15 (td, 13H, *J* = 7.0, 3.4 Hz). ^{13}C NMR (75 MHz, $CDCl_3$) δ 170.6, 169.9, 153.8, 153.5, 153.3, 149.2, 133.5, 130.5, 129.0, 128.6, 124.2, 123.1, 108.6, 108.0, 103.5, 98.0, 77.3, 77.0, 76.8, 67.9, 57.3, 44.4, 30.5, 29.5, 14.9, 12.5. ESI-MS C33H40N3O4S Exact Mass: 574.2740，Found: 574.2736 ($[M+H]^+$).

2.4 Cell culture

MCF-7 (human breast carcinoma) were obtained from Institute of Basic Medical Sciences (IBMS) of Chinese Academy of Medical Sciences (CAMS) and cultured in RPMI 1640 supplemented with 10% FBS (fetal bovine serum) in an atmosphere of 5% CO_2 and 95% air at 37 °C. Grow MCF-7 Cells in the exponential phase of growth on 35-mm glass-bottom culture dishes (Φ 20 mm) for 1-2 days to reach 70-90% confluency. The cells was washed three times with RPMI 1640, and then incubated for 10 min in an atmosphere of 5% CO_2 and 95% air at 37 °C with 2 mL RPMI 1640 containing a certain concentration of fluorescent probe. Wash cells twice with 1 mL PBS at room temperature, and then add 1 mL RPMI 1640 culture medium and observe under a confocal microscopy.

3. Results and Discussion

3.1 Synthesis

As shown in Scheme 2, a two-step-in-one-pot synthesis of Rh-MM was very concise and highly efficient. Reaction of rhodamine B with $POCl_3$ followed by the L-methionine methyl ester afforded Rh-MM with 62% yield. In the presence of 10 equiv NaOH, Rh-MM was hydrolyzed to afford Rh-Met with 82% yield.

3.2 Spectral responses of Rh-Met vs different pH values

The spectral response to pH was studied to confirm the pKa value of Rh-Met. Rh-Met showed no absorption in C_2H_5OH-H_2O (v,v 1:9) solution

when the pH value was above 9.16. With the addition of hydrochloric acid, a new absorption peak observed at 563 nm was significantly enhanced (Fig. S1, ESI). Meanwhile, the color of

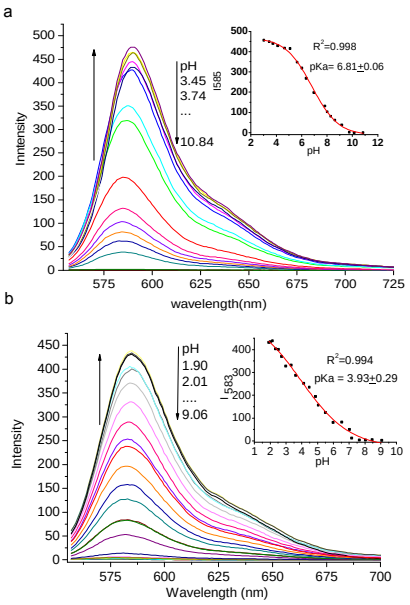

Fig. 1 Emission-spectral changes of (a) Rh-Met (3 μM, C_2H_5OH:H_2O, 1/9, v/v) and (b) Rh-MM (2 μM, C_2H_5OH:H_2O, 2/3, v/v) vs different pH values. Inset graph: intensity at emission maximum as a function of pH values.

the solution also turned from colorless to pink, indicating that spirolactam underwent a ring-opening reaction in the process of protonation of Rh-Met. Upon titrating of hydrochloric acid, emission spectral changes were observed as shown in Fig. 1a. Probe Rh-Met showed a significant fluorescence enhanced signal (240-fold enhancement of fluorescence intensity at 585 nm) with attenuation of pH values from 9.7 to 3.5. The fluorescence titration data provided the pKa of probe Rh-Met as 6.81 (±0.06) (Fig. 1a), which was much higher than that of Rh-MM (pKa 3.93 (±0.29)) (Fig.1b). Compared with Rh-MM, the carboxylate moiety of Rh-Met is relatively more alkaline than the ester group in Rh-MM. Neutral pKa of Rh-Met can be ascribed to the protonation of carboxylate and hydrogen bonding formation. Furthermore, a highly steric group of bulky formylmethinione moiety may also play a vital role in tuning the pka of Rh-Met [32].

3.3 Selectivity of Rh-Met to H^+ over other metal ions and biological relevant species

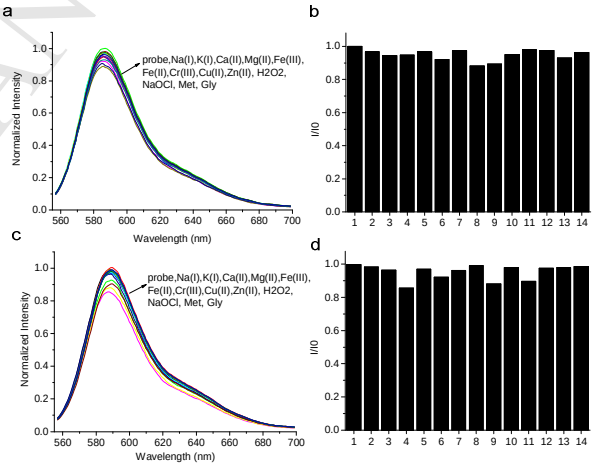

Fig. 2 Normalized fluorescent intensity at 585 nm of Rh-Met (5 μM) in the absence and presence of different metal ions and biological relevant species at pH 7.4 (a,b) and 4.5 (c,d). (b)1:pH7.4, (d)1:pH4.5, 2:Na^+, 3:K^+, 4:Fe^{2+}, 5:Mg^{2+}, 6:Zn^{2+}, 7:Ca^{2+}, 8:Cu^{2+}, 9:Fe^{3+}, 10:Cr^{3+}, 11:H_2O_2, 12:NaOCl, 13:Methione, 14:Glycine

Competitive experiments in the presence of common metal ions and biological relevant species were used to examine the effect on pH measurement. In a phosphate buffer solution with

pH 7.4 (C_2H_5OH:buffer, 1/9, v/v), the presence of 10 equiv various metal ions and biological relevant species, such as K^+, Ca^{2+}, Na^+, Mg^{2+}, Fe^{2+}, Fe^{3+}, Cu^{2+}, Zn^{2+}, Cr^{3+}, H_2O_2, NaOCl, Methinione, Glycine, didn't cause any observable spectral changes (Fig. 2a,2b), indicating that the ring-opening reaction of spirolactam of Rh-Met was not brought about by presence of these species at neutral pH. In order to further assess the effect of these species on pH measurement in acidity conditions, these species were added into a phosphate buffer solution with pH 4.5 (Rh-Met 5 μM, C_2H_5OH:buffer, 1/9, v/v). As shown in Fig. 2c, the strong emission of Rh-Met was not obstructed by the addition of 10 equiv various species (Fig. 2d). The spectral responses of major metal ions such as Na^+, K^+ and Ca^{2+} at physiological concentrations were also investigated (Fig. S3). These results suggested that probe Rh-Met exhibited a high selectivity to hydrogen ion, and had potential to be used as a neutral fluorescent probe in biological imaging.

3.4 Reversibility of the response of Rh-Met to H^+

In addition to high selectivity, Rh-Met also exhibited a good reversible response to hydrogen ion, which was verified by fluorescence titration experiment of Rh-Met in aqueous solution (C_2H_5OH: H_2O, 1/9, v/v) at pH values ranging from alkaline to acidic by the alternating addition of hydrochloric acid and sodium hydroxide. As illustrated in Fig 3a, upon adjusting the pH value of the solution to acidic (~ 4.6), a color change of solution from colourless to pink became immediately visible to the naked-eyes and a red emission at 585 nm was detected (quantum yield Φ 0.51 at pH 4.5), whereas when the pH value was up at 7.2-8.6, both the color and fluorescence of Rh-Met disappeared (Fig 3b). Rh-Met exhibited a remarkably higher reversibility towards H^+, which indicated that Rh-Met had the potential to be a useful tool for rapid measurement of pH values.

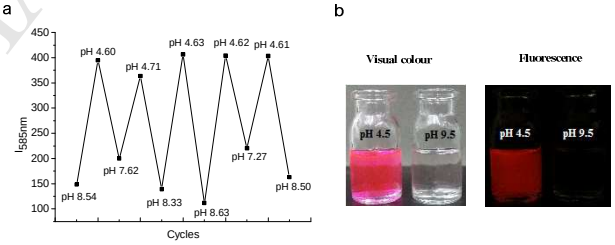

Fig. 3 (a) Fluorescent intensity at 585 nm of Rh-Met (3 μM) in C_2H_5OH: H_2O (1/9, v/v) solution at different pH values by the alternating addition of HCl and NaOH. (b)Visual colour and fluorescent Image of Rh-Met (3 μM) in C_2H_5OH: H_2O (1/9, v/v) solution at pH 4.5 and 9.5, respectively.

3.5 Laser scanning confocal fluorescent imaging of Rh-Met

The characteristic negative charge of Rh-Met in neutral aqueous solution may make Rh-Met tend to accumulate in mitochondria of cells. Therefore Rh-Met was applied for biological imaging in cultured MCF-7 by using a confocal laser scanning

microscopy. Upon excitation at 559 nm, red intracellular fluorescence (red channel BF:565-665nm) was distributed in discrete subcellular locations of cells (Fig. 4a-4c), which suggested that probe Rh-Met with negative charge could permeate into cells. In order to validate whether probe Rh-Met can be directionally accumulated in mitochondria of cells, co-localization experiments were performed by co-staining MCF-7 cells with 2 μM 3,6-diamino-9-[2-(methoxy-carbonyl)phenyl]-xanthylium chloride (rhodamine 123, Rh123), a mitochondria tracker. MCF-7 cells showed green and red fluorescence in Channel 1 and 2(Fig. 4d, Ch1 and Ch2), respectively, after staining with 5 μM Rh-Met and 2 μM Rh123 for 10 minutes. The image of Ch2 merged well with the image staining with Rh123 (Ch1) (Fig. 4e,) indicating that Rh-Met can specifically localize in mitochondria of living cells. Intensity profile of linear ROI across MCF-7 cells stained with Rh-Met and Rh123 also varied in close synchrony (Fig. 4f). High Pearson's coefficient and overlap coefficient were 0.900 and 0.993, respectively, evaluated using conventional dye-overlay method [37].

During the experiment of cellular staining, it was also found that probe Rh-Met could be directionally accumulated not only in mitochondria but also in lipid droplets. As illustrated in Fig. 5a, except for

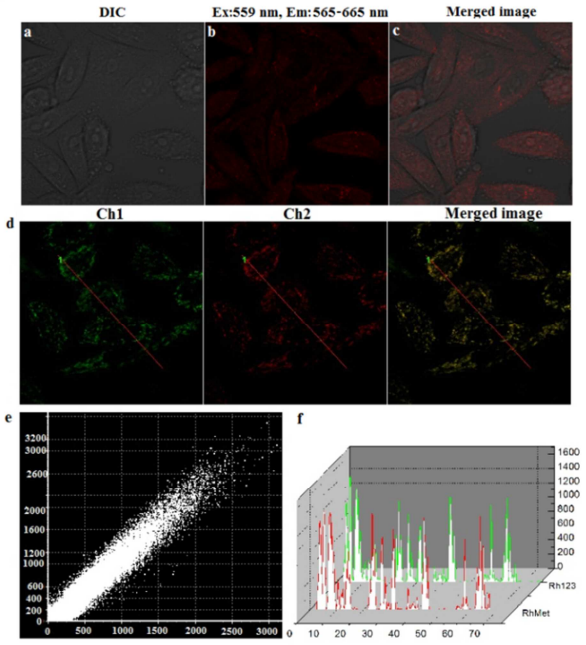

Fig. 4 (a) Fluorescent images of MCF-7 cells stained with Rh-Met (5 μM). DIC: differential interference contrast, (b) Fluorescent image: λex 559 nm, λem 565-665 nm, (c) Merged image is overlay of DIC and fluorescent image. (d) Fluorescent image of MCF-7 cells co-stained with Rh-Met (5 μM) and Rh123 (2 μM). Ch 1 (Channel 1): λex 488 nm, λem 495-535 nm), Ch2 (Channel 2): λex 559 nm, λem 565-665 nm, Merged image is overlay of Ch1 and Ch2. (e) Intensity correlation plot of stain Rh-Met and Rh123. (f) Intensity profile of region of interest (ROI, red line) cross MCF-7 cells

weak fluorescence in cellular mitochondria, there were a lot of discrete spots with strong red fluorescence in cells stained with Rh-Met. To further confirm the dot organells, co-localization experiments were performed by co-staining MCF-7 cells with 4,4-Difluoro-1,3,5,7,8-Pentamethyl-4-Bora-3a,4a-Diaza-s-Indacene(BODIPY®493/503), a lipid droplets tracker. As shown in Fig. 5b, in Ch 1 MCF-7 cells stained with BODIPY®493/503

exhibited a strong fluorescence in lipid droplets, while in Ch 2, MCF-7 cells stained with Rh-Met showed a significant red fluorescence in lipid droplets and a weak fluorescence in mitochondria. The image of Ch2 merged well with the image staining stained with BODIPY®493/503 (Ch1). These results indicated that Rh-Met may tend to accumulate in lipid droplets in a certain growth stage of living cells. It was interesting that Rh-Met accumulating in lipid droplets displayed a strong red fluorescence. In order to determine the effect of polarity on the fluorescence properties of Rh-Met, the solvent effect of Rh-Met was investigated (Fig S4). Absorption and emission

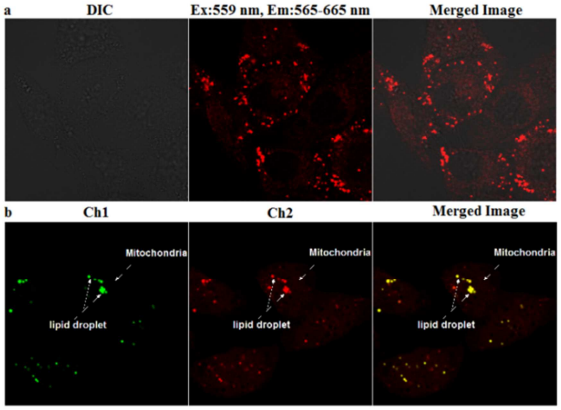

Fig. 5 (a) Fluorescent images of MCF-7 cells stained with Rh-Met (5 μM). DIC: differential interference contrast, Fluorescent image: λex 559 nm, λem 565-665 nm, merged image is overlay of DIC and fluorescent image. (b) Fluorescent image of MCF-7 cells co-stained with Rh-Met (5 μM) and BODIPY®493/503 (5 μM). Ch 1 (Channel 1): λex 488 nm, λem 495-535 nm), Ch2 (Channel 2): λex 559 nm, λem 565-665 nm, Merged image is overlay of Ch1 and Ch2.

spectra of Rh-Met were obtained in solvents such as dichloromethane, ethyl acetate, tetrahydrofuran, methanol and N,N-dimethylamino formamide, respectively (Fig S4). In methanol and dichloromethane, the maximum absorption of Rh-met was much lower than that of Rh-Met under acidic condition, but relatively higher than that of Rh-Met in THF, DMF and AcOEt. These results indicated that the polarity of solvent was not the main factor affecting the ring-opening reaction of Rh-Met. Hence it is inclined that the fluorescence signal from lipid droplet may be due to the local acidity rather than the lipophilic nature of the droplet. The possible reason may be that phosphatidic acid, as a transient intermediate in lipid biosynthesis, may cause the pH to fluctuate in lipid droplets [38,39]. Laser scanning confocal microscopy experiments of MCF-7 cells approved showed that Rh-Met would be a potential fluorescent probe to assess the pH values and reveal the relationship between mitochondria and lipid droplets.

In order to further determine the feasibility of monitoring pH fluctuation of Rh-Met in living cells, acid stimulating experiment was used to perturb the cellular pH and demonstrate the changes of fluorescence signal in living cells. Upon excitation at 559 nm, red intracellular fluorescence was distributed in MCF-7 cells in the absence of acetic

acid as a stimulant, as shown in Fig 6a. Upon addition of acetic acid (10 equiv.), the MCF-7 cells displayed measurable levels of red fluorescence in discrete subcellular locations, as shown in Fig 6b. These results indicated that Rh-Met could report the fluctuation of pH in mitochondria of living cells in the presence of induction drug.

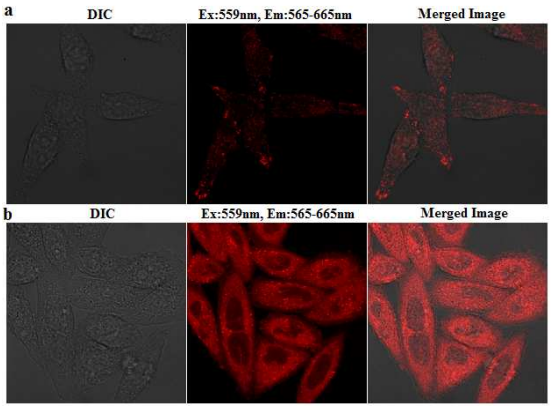

Fig. 6 (a) DIC image, fluorescent image and merged image of MCF-7 cells stained with Rh-Met (5.0 μM) (b) DIC image, fluorescent image and merged image of MCF-7 cells stained with Rh-Met (5.0 μM) and acetic acid (10 equiv.)

4. Conclusions

In summary, we have developed a neutral pH fluorescent probe (Rh-Met) based on rhodamine spirolactam bearing L-methionine moiety. Rh-Met exhibited a 240-fold enhancement of fluorescence intensity at 585 nm with attenuation of pH values from 9.7 to 3.5. The pKa value of Rh-Met was 6.81(±0.06) and higher than that of other rhodamine spirolactams known, which can be attributed to a stabilization of hydrogen bonding formation in ring-opening reaction of spirolactam. Rh-Met displayed an excellent selectivity and reversible response to hydrogen ion. Rh-Met was successfully employed for imaging endocellular hydrogen ion in mitochondria and lipid droplets, suggesting that Rh-Met could be a potential tool to assess pH fluctuation in mitochondria and lipid droplets. It is anticipated that this new probe will further reveal the relationship between mitochondria and lipid droplets, and promote many new opportunities for studying the biological effect of pH in living cells.

Acknowledgments

This work was supported by National Natural Science Foundation of China (No. 21302080), Program Funded by Liaoning Province Education Administration (No. L2014010) and National Water Pollution Control and Treatment Science and Technology Major Project (2015ZX07202012).

References

[1] Warde L G, Jr. *Organic Chemistry*, 2nd. Ed., 1991, p892-893.

[2] Morisawa Y, Yasunaga M, Sato H, Fukuda R, Ehara M, Ozaki Y. Rydberg and π-π transitions in film surfaces of various kinds of nylons studied by attenuated total reflection far-ultraviolet spectroscopy and quantum chemical calculations: peak shifts in the spectra and their relation to nylon structure and hydrogen bondings. J Phys Chem B 2014; 118:11855-11861.

[3] Cowan ML, Bruner BD, Huse N, Dwyer JR, Chugh B,

Nibbering ET, Elsaesser T, Miller RJ. Ultrafast memory loss and energy redistribution in the hydrogen bond network of liquid H_2O. Nature 2005; 434:199-202.

[4] Politi R, Harries D: Enthalpically driven peptide stabilization by protective osmolytes. Chem Commun 2010;46:6449-6451.

[5] Shokri A, Abedin A, Fattahi A, Kass SR. Effect of hydrogen bonds on pKa values: importance of networking. J Am Chem Soc 2012;134:10646-10650.

[6] Beija M, Afonso CA, Martinho JM. Synthesis and applications of Rhodamine derivatives as fluorescent probes. Chem Soc Rev 2009;38:2410-2433.

[7] Kim HN, Lee MH, Kim HJ, Kim JS, Yoon J. A new trend in rhodamine-based chemosensors: application of spirolactam ring-opening to sensing ions. Chem Soc Rev 2008;37:1465-1472.

[8] Kwon J, Jang Y, Lee Y, Kim K, Seo M, Nam W, Yoon J. A Highly Selective Fluorescent Chemosensor for Pb^{2+}. J Am Chem Soc 2005;127:10107-10111

[9] Zheng H, Qian ZH, Xu L, Yuan FF, Lan LD, Xu JG: Switching the recognition preference of rhodamine B spirolactam by replacing one atom: design of rhodamine B thiohydrazide for recognition of Hg(II) in aqueous solution. Org Lett 2006, 8:859-861.

[10] Zheng H, Shang GQ, Yang SY, Gao X, Xu JG: Fluorogenic and chromogenic rhodamine spirolactam based probe for nitric oxide by spiro ring opening reaction. Org Lett 2008, 10:2357-2360.

[11] Sasaki H, Hanaoka K, Urano Y, Terai T, Nagano T: Design and synthesis of a novel fluorescence probe for Zn2+ based on the spirolactam ring-opening process of rhodamine derivatives. Bioorg Med Chem 2011, 19:1072-1078.

[12] Sakabe M, Asanuma D, Kamiya M, Iwatate RJ, Hanaoka K, Terai T, Nagano T, Urano Y: Rational design of highly sensitive fluorescence probes for protease and glycosidase based on precisely controlled spirocyclization. J Am Chem Soc 2013, 135:409-414.

[13] Lee MK, Rai P, Williams J, Twieg RJ, Moerner WE: Small-molecule labeling of live cell surfaces for three-dimensional super-resolution microscopy. J Am Chem Soc 2014, 136:14003-14006.

[14] Dujols V, Ford F, Czarnik AW. A Long-Wavelength Fluorescent Chemodosimeter Selective for Cu(II) Ion in Water. J Am Chem Soc 1997;119:7386-7387

[15] Zheng H, Shang GQ, Yang SY, Gao X, Xu JG. Fluorogenic and chromogenic rhodamine spirolactam based probe for nitric oxide by spiro ring opening reaction. Org Lett 2008;10:2357-2360.

[16] Egorova OA, Seo H, Chatterjee A, Ahn KH. Reaction-based fluorescent sensing of Au(I)/Au(III) species: mechanistic implications on vinylgold intermediates. Org Lett 2010;12:401-403.

[17] Yu H, Zhang X, Xiao Y, Zou W, Wang L, Jin L. Targetable fluorescent probe for monitoring exogenous and endogenous NO in mitochondria of living cells. Anal Chem 2013;85:7076-7084.

[18] Kim H, Lee S, Lee J, Tae J. Rhodamine triazole-based fluorescent probe for the detection of Pt(2+). Org Lett 2010;12:5342-5345.

[19] Du P, Lippard SJ. A highly selective turn-on colorimetric, red fluorescent sensor for detecting mobile zinc in living cells. Inorg Chem 2010;49:10753-10755.

[20] Yang Z, She M, Yin B, Cui J, Zhang Y, Sun W, Li J, Shi Z. Three rhodamine-based "off-on" chemosensors with high selectivity and sensitivity for Fe3+ imaging in living cells. J Org Chem 2012;77:1143-1147.

[21] Long L, Lin W, Chen B, Gao W, Yuan L. Construction of a FRET-based ratiometric fluorescent thiol probe. Chem

Commun 2011; 47:893-895.

[22] Kumar M, Kumar N, Bhalla V, Singh H, Sharma PR, Kaur T. Naphthalimide appended rhodamine derivative: through bond energy transfer for sensing of Hg2+ ions. Org Lett 2011;13:1422-1425.

[23] Li H, Fan J, Wang J, Tian M, Du J, Sun S, Sun P, Peng X. A fluorescent chemodosimeter specific for cysteine: effective discrimination of cysteine from homocysteine. Chem Commun 2009;39:5904-5906.

[24] Huang W, Zhou P, Yan W, He C, Xiong L, Li F, Duan C. A bright water-compatible sugar-rhodamine fluorescence sensor for selective detection of Hg^{2+} in natural water and living cells. J Environ Monit 2009;11:330-335.

[25] Zhao Y, Zhang XB, Han ZX, Qiao L, Li CY, Jian LX, Shen GL, Yu RQ. Highly sensitive and selective colorimetric and off-on fluorescent chemosensor for Cu2+ in aqueous solution and living cells. Anal Chem 2009;81:7022-7030.

[26] Wang E, Zhou Y, Huang Q, Pang L, Qiao H, Yu F, Gao B, Zhang J, Min Y, Ma T. 5-Hydroxymethylfurfural modified rhodamine B dual-function derivative: Highly sensitive and selective optical detection of pH and Cu(2+). Spectrochim Acta A Mol Biomol Spectrosc 2016;152:327-335.

[27] Zhang W, Tang B, Liu X, Liu Y, Xu K, Ma J, Tong L, Yang G. A highly sensitive acidic pH fluorescent probe and its application to HepG2 cells. Analyst 2009;134:367-371.

[28] Hasegawa T, Kondo Y, Koizumi Y, Sugiyama T, Takeda A, Ito S, Hamada F. A highly sensitive probe detecting low pH area of HeLa cells based on rhodamine B modified beta-cyclodextrins. Bioorg Med Chem 2009;17(16):6015-6019.

[29] Bojinov VB, Venkova AI, Georgiev NI. Synthesis and energy-transfer properties of fluorescence sensing bichromophoric system based on Rhodamine 6G and 1,8-naphthalimide. Sensor Actuat B Chem 2009;143: 42-49

[30] Hua ZQ, Li M, Liu MD, Zhuang WM, Li GK. A highly sensitive fluorescent acidic pH probe based on rhodamine B diethyl-2-aminobutenedioate conjugate and its application in living cells. Dyes Pigments 2013; 96:71-75.

[31] Wang E, Zhou Y, Huang Q, Pang L, Qiao H, Yu F, Gao B, Zhang J, Min Y, Ma T. 5-Hydroxymethylfurfural modified rhodamine B dual-function derivative: Highly sensitive and selective optical detection of pH and Cu(2+). Spectrochim Acta A Mol Biomol Spectrosc 2016;152:327-335.

[32] Yuan L, Lin W, Feng Y. A rational approach to tuning the pKa values of rhodamines for living cell fluorescence imaging. Org Biomol Chem 2011;9:1723-1726.

[33] Lv HS, Huang SY, Zhao BX, Miao JY. A new rhodamine B-based lysosomal pH fluorescent indicator. Anal Chim Acta 2013;788:177-182.

[34] Zhu H, Fan J, Xu Q, Li H, Wang J, Gao P, Peng X. Imaging of lysosomal pH changes with a fluorescent sensor containing a novel lysosome-locating group. Chem Commun 2012;48:11766-11768.

[35] Li H, Wang C, She M, Zhu Y, Zhang J, Yang Z, Liu P, Wang Y, Li J. Two rhodamine lactam modulated lysosome-targetable fluorescence probes for sensitively and selectively monitoring subcellular organelle pH change. Anal Chim Acta 2015;900:97-102.

[36] Yu KK, Hou JT, Li K, Yao Q, Yang J, Wu MY, Xie YM, Yu XQ. A single design strategy for dual sensitive pH probe with a suitable range to map pH in living cells. Sci Rep 2015;5:15540-15550.

[37] Yu H, Xiao Y, Jin L. A lysosome-targetable and two-photon fluorescent probe for monitoring endogenous and exogenous nitric oxide in living cells. J Am Chem Soc 2012;134(42):17486-17489.

[38] Kemmer GC, Bogh SA, Urban M, Palmgren MG, Vosch T, Schiller J, Gunther Pomorski T. Lipid-conjugated fluorescent pH sensors for monitoring pH changes in reconstituted membrane systems. Analyst 2015;140: 6313-6320.

[39] Penno A, Hackenbroich G, Thiele C. Phospholipids and lipid droplets. Biochim Biophys Acta 2013;1831: 589-594.

Highlights:

1. A neutral pH probe inspired by effect of hydrogen bond on pKa was developed.
2. The pKa of probe was 6.81 and higher than that of other rhodamine spirolactams known.
3. Probe displayed an excellent selectivity, organelle-targeting.
4. It would be a potential tool to assess pH fluctuation in mitochondria of live cells.